SANDIA REPORT
SAND2009-6096
Unlimited Release
Printed October 2009

Surface Plasmon Sensing of Gas Phase Contaminants Using Optical Fiber

Kent B. Pfeifer, Steven M. Thornberg, Michael I. White, Arthur N. Rumpf

Prepared by
Sandia National Laboratories
Albuquerque, New Mexico 87185 and Livermore, California 94550

Sandia is a multiprogram laboratory operated by Sandia Corporation,
a Lockheed Martin Company, for the United States Department of Energy's
National Nuclear Security Administration under Contract DE-AC04-94AL85000.

Approved for public release; further dissemination unlimited.

Sandia National Laboratories

Issued by Sandia National Laboratories, operated for the United States Department of Energy by Sandia Corporation.

NOTICE: This report was prepared as an account of work sponsored by an agency of the United States Government. Neither the United States Government, nor any agency thereof, nor any of their employees, nor any of their contractors, subcontractors, or their employees, make any warranty, express or implied, or assume any legal liability or responsibility for the accuracy, completeness, or usefulness of any information, apparatus, product, or process disclosed, or represent that its use would not infringe privately owned rights. Reference herein to any specific commercial product, process, or service by trade name, trademark, manufacturer, or otherwise, does not necessarily constitute or imply its endorsement, recommendation, or favoring by the United States Government, any agency thereof, or any of their contractors or subcontractors. The views and opinions expressed herein do not necessarily state or reflect those of the United States Government, any agency thereof, or any of their contractors.

Printed in the United States of America. This report has been reproduced directly from the best available copy.

Available to DOE and DOE contractors from
U.S. Department of Energy
Office of Scientific and Technical Information
P.O. Box 62
Oak Ridge, TN 37831

Telephone: (865) 576-8401
Facsimile: (865) 576-5728
E-Mail: reports@adonis.osti.gov
Online ordering: http://www.osti.gov/bridge

Available to the public from
U.S. Department of Commerce
National Technical Information Service
5285 Port Royal Rd.
Springfield, VA 22161

Telephone: (800) 553-6847
Facsimile: (703) 605-6900
E-Mail: orders@ntis.fedworld.gov
Online order: http://www.ntis.gov/help/ordermethods.asp?loc=7-4-0#online

SAND2009-6096
Unlimited Release
Printed October 2009

Surface Plasmon Sensing of Gas Phase Contaminants Using Optical Fiber

[a]Kent B. Pfeifer, [b]Steven M. Thornberg, [b]Michael I. White, [a]Arthur N. Rumpf
[a]Integrated Microdevice Systems, 1717
[b]Materials Reliability, 1825
Sandia National Laboratories
PO Box 5800
Albuquerque, New Mexico 87185-1717

Abstract

Fiber-optic gas phase surface plasmon resonance (SPR) detection of several contaminant gases of interest to state-of-health monitoring in high-consequence sealed systems has been demonstrated. These contaminant gases include H_2, H_2S, and moisture using a single-ended optical fiber mode. Data demonstrate that results can be obtained and sensitivity is adequate in a dosimetric mode that allows periodic monitoring of system atmospheres. Modeling studies were performed to direct the design of the sensor probe for optimized dimensions and to allow simultaneous monitoring of several constituents with a single sensor fiber. Testing of the system demonstrates the ability to detect 70mTorr partial pressures of H_2 using this technique and <280 μTorr partial pressures of H_2S. In addition, a multiple sensor fiber has been demonstrated that allows a single fiber to measure H_2, H_2S, and H_2O without changing the fiber or the analytical system.

ACKNOWLEDGMENTS

The authors would like to acknowledge Sandia's Laboratory Directed Research and Development (LDRD) program for supporting this work. Sandia is a multiprogram laboratory operated by Sandia Corporation, a Lockheed Martin Company for the United States Department of Energy's National Nuclear Security Administration under contract DE-AC04-94AL85000.

CONTENTS

Acknowledgments 4

Contents 5

Figures 6

1. Introduction 7

2.Theory: 8

3. Modeling Results: 10

4. Experimental 11
Preparation of the Fiber 11

5. MATLAB Algorithms 12

6. Results 12
Pd/H2 12
Ag/H2S 13
SiO2/H2O 13

7. Multi Coating SPR Fiber 13

8. Conclusions 14

9. References 14

10. Distribution 24

FIGURES

Figure 1. Schematic diagram of the SPR sensor showing the optical system. Broad band light is injected into the fiber which then is sent to the SPR end via a three-port coupler. The light is passed through the SPR section of the fiber and reflected back by a retro-reflecting end back through the coupler and is detected by the monochromator. 15

Figure 2. Diagram of geometry used to derive equations where the subscript 0 represents the outside atmosphere, 1 is the SPR supporting metal layer, 2 is the core, and 3 is an optional second transduction layer. 16

Figure 3. Plot of calculated reflectance for several thicknesses of Pd film exposed to H_2 to form PdH_x as calculated and compared to an unexposed 12.5 mm length, 20 nm thick Pd film in the SPR geometry. Data indicate that good candidates for fabrication and testing due to their broad absorption resonance being predicted in the 250-400 nm range are films with thicknesses of 20-40 nm . The real and imaginary parts of the index of refraction were obtained from the literature for PdH_x and are plotted in the inset graph.[17,18] 17

Figure 4. Plot of optical transmission for a 20 nm Au coated fiber as a function of wavelength for several different core diameters using the theory of Xu *et al.*[7] Plot illustrates that for SPR, the larger diameter gives a narrower SPR peak allowing more wavelength discrimination. 18

Figure 5. Plot of the raw spectral response from a 30 nm Pd coated fiber under conditions of near vacuum pumped from an air background and exposed to ~0.2 Torr of H_2. 19

Figure 6. Plot of the normalized response of a 40 nm Pd film with a 100 nm Au retroreflector as a function of H_2 partial pressure at several wavelengths indicating that the sign of the response is wavelength dependent. Limit of detection on the order of 70 mTorr of H_2.. 20

Figure 7. Plot of sensor response as a function of wavelength and scan time plotted along with the H2 partial pressure. Data illustrate that the sensor is reversible and has a strong dependence on wavelength as expected. 21

Figure 8. Diagram of three section SPR sensor showing Au, Ag, and Pd regions on a 600 µm optical fiber core. 22

Figure 9. Plot showing the response to 200 mTorr H_2 in Pd (a), 280 µTorr H_2S on Ag (b), 200 mTorr H_2 in Pd (c), and drying the fiber from 0˚C frost point to -70˚C frost point (d) on a single SPR fiber. The time progression is from top to bottom and the data is re-normalized after the H_2S on Ag exposure since that change is not reversible. Thus, (c) and (d) are normalized to (b). The SPR wavelengths are separated with the minimum for Ag at approximately 450 nm, the minimum for Pd at about 550 nm, and the minimum for Au at about 600 nm. The dotted lines locate the minimum of the smoothed data. 23

1. INTRODUCTION

Surface plasmon resonance spectroscopy (SPR) has been applied to a number of analytical problems due to its high sensitivity to variations in the electronic nature of a surface. In particular, reports of sensing of chemicals and of biological samples using functionalized surfaces are widespread in the literature.[1,2,3,4,5,6] However, the majority of examples employ an optical arrangement known as a Kretschmann configuration that has a single angle of incidence on a metallic layer and a single angle of exit to an optical spectrometer. The surface plasmon resonance is supported in a thin metallic layer and the chemistry of interest takes place on the side of the metal layer opposite the incident and reflected light. In practice this thin metallic layer is usually deposited on the diagonal facet of a right-angle prism allowing the thin film access to the chemical system while having structural support for the film provided by the prism.

For SPR measurements in a laboratory setting where the geometry of the optical system can be conveniently constructed, the Kretschmann configuration is optimum due to the narrow resonances measured. However, for monitoring of sealed systems in field environments where internal volume and external access is limited by the general function of the system, the Kretschmann geometry is often difficult or impossible to implement. For such systems optical fiber based SPR systems have been applied. An optical fiber-based SPR sensor is normally made from a single fiber that has its cladding etched down to the optical core of the fiber over a known section of length. The exposed core is then coated with an SPR supporting metal and the sensor is used in a single-pass configuration.[7,8,9] A fundamental difference between an optical fiber and the common Kretschmann configuration is that in a multimode optical fiber, the allowed incident angles are a continuum from the critical angle of the fiber as set by the numerical aperture to $\pi/2$ from normal. As has been demonstrated both experimentally and theoretically, this has the effect of significantly broadening the SPR peak.[7,8]

A single-fiber version of the fiber-optic SPR sensor that employs a retro-reflecting metal film on the end of a multimode fiber similar in geometry (Figure 1) to the intensity-based "micromirror" sensors documented in the literature has been demonstrated. [10,11,12,13] While the geometry is similar to previous work, the previous work only sampled the reflectance of the reflecting mirror on the fiber. In our system, light is injected into the fiber that then travels by way of the optical coupler to the SPR coated fiber where it interacts with the sensing film. The light is then retro-reflected back through the fiber to the coupler where half returns to the light source and is lost and the other half is directed via the second leg of the coupler to the monochrometer where it is analyzed. The reflecting end serves the purpose of returning the light back through the fiber to the monochromator but does not participate in the sensing. This is accomplished by making the end from an inert noble metal such as Au or overcoating the metal with a sealant.

Since the fiber is single ended, it becomes practical to use this sensor to monitor the atmospheres of complex subsystems for contamination and aging effects. For example, deterioration of some important compounds found in packaging can lead to production of sulfur compounds that can corrode connectors and lead to electronic failures. In addition, in sealed systems, batteries can sometimes evolve H_2 leading to metallic embrittlement. Further, leakage of seals can allow moisture to infiltrate and condense on critical components contributing to corrosion and other failure mechanisms.

2. THEORY:

The numerical model was used to determine the approximate thickness for the SPR films required. These calculations were accomplished using the 600 μm core fused quartz fiber and assuming that the index of refraction was constant over the spectral range of 250 nm to 1000 nm at a value of $n_q \cong 1.46$ and a numerical aperture of $NA=0.22$. Comparison to the fiber data sheet confirms the validity of this constant assumption to within 3% over this wavelength range. These quantities allow the calculation of the critical angle in the fiber which establishes the lower limit of integration in the model as follows:[14]

$$\theta_c = \frac{\pi}{2} - \sin^{-1}\left(\frac{NA}{n_q}\right) \qquad [1]$$

For a single pass system with no retro-reflector, the reflectance *(R)* as a function of wavelength *(λ)* of the SPR surface is given where $p(\theta)$ is the incident power on the film at the angle θ, $r^N(\theta)$ is the reflectance for each individual ray at the angle θ, N is the number of reflections from the surface as determined by the incident angle and the length of the SPR supporting metal (L), and λ is the wavelength of the light.

$$R(\lambda) = \frac{\int_{\theta_c}^{\pi/2} p(\theta) r^N(\theta) d\theta}{\int_{\theta_c}^{\pi/2} p(\theta)\, d\theta} \qquad [2]$$

$$N = \frac{L}{d_2 \tan(\theta)}$$

A complete description of the method is outlined in detail in Xu *et al*.[7] In Eq. [2], the argument of the numerator integral is the power that remains after multiple reflections of any single transverse magnetic (TM) ray at any single angle θ. Recognizing that this a continuum of rays, integration was performed on the guided rays from the critical angle θ_c below which the light will be lost to fiber cladding leakage into the fiber to an angle of incidence of π/2 (grazing incidence with the core cladding interface). A Lambertian model was employed for our light source to model the tungsten-halogen lamp used to illuminate our sample fibers. A Lambertian source has the property of having a uniform radiance that is independent of the angle into which the radiation is directed (Ocean Optics LS-1).[15] Thus, the optical power can be expressed as the function:[7]

$$p(\theta) = p_o\, n_q^2 \sin\theta \cos\theta \qquad [3]$$

In Eq. [3], p_o is the nominal power from the light source. Since the power function appears in both the numerator and the denominator of Eq. [2], the absolute magnitude of the power is normalized leaving only the ratio of the reflected light to the incident light or the reflectance of the fiber-film system.

A fundamental concept of SPR is that surface plasmon resonance can only be varied for the TM (transverse magnetic) polarized light as a function of angle; thus, the transmission through a coated section of fiber must be expressed as the following:

$$T(\lambda) = \frac{\Phi_{TE} + R(\theta)\Phi_{TM}}{\Phi_{total}} = \frac{1}{2} + \frac{R(\theta)}{2} \qquad [4]$$

In Eq. [4], Φ is the transmitted optical power in each of the TM and TE (transverse electric) modes. Light is assumed to be evenly distributed between the two modes resulting in half the transmission coming from the TE mode that is undisturbed by SPR, and the rest coming from the total reflection from the coating divided by two since only half of the original incident light can participate in SPR.

A double pass optical configuration was employed as shown in Figure **1** which requires a metallic film to be deposited on the end facet of the fiber to retro-reflect the light back toward the detector. Thus, an additional correction to $T(\lambda)$ must be made to compensate for the spectral influence of the retro-reflector on the incident light. Thus, again assuming that half the light is TE mode and does not contribute to SPR but is modified by the retro-reflector according to Fresnel's equations and the other half of the light is modified both by the SPR and the retro-reflecting surface Eqs. [2] and [4] can be modified as follows:

$$T(\lambda) = \frac{1}{2}\frac{\int_{\theta_c}^{\pi/2} p(\theta) R_{TE}(\theta) d\theta}{\int_{\theta_c}^{\pi/2} p(\theta)\, d\theta} + \frac{1}{2}\frac{\int_{\theta_c}^{\pi/2} p(\theta)\ R_{TM}(\theta) d\theta}{\int_{\theta_c}^{\pi/2} p(\theta)\, d\theta} \qquad [5]$$

where R_{TE} is defined as:[16]

$$R_{TE}(\theta) = \left(\frac{n_2 \cos\theta_i - n_{rr}\cos\theta_t}{n_2 \cos\theta_i + n_{rr}\cos\theta_t}\right)^2 \left(\frac{n_2 \cos\theta - n_1 \cos\theta'}{n_2 \cos\theta + n_1 \cos\theta'}\right)^{4N} \qquad [6]$$

and R_{TM} is defined as:

$$R_{TM}(\theta) = \left(\frac{n_{rr}\cos\theta_i - n_2 \cos\theta_t}{n_{rr}\cos\theta_i + n_2 \cos\theta_t}\right)^2 r^{2N}(\theta) \qquad [7]$$

The angles in Eqs. [6] and [7] are defined in Figure 2. In Eq. [6], the left-hand term is the Fresnel equation for light polarized such that the electric field is perpendicular to the plane of incidence or TE as defined above for the single reflection off of the retro-reflector. The right-hand term is the same Fresnel equation configured for the multiple reflections off of the fiber core to SPR film interface again in TE mode. Note this term is raised to the *4N* rather than *2N* power because the length of the SPR supporting metal is twice as long due to the double pass nature of the fiber architecture and there are *N* individual reflections in each direction. The right-hand term in Eq. [7] is the SPR term derived by Xu et al. (Eq. [9]) and the left-hand term is the Fresnel equation for reflection off of the retro-reflector for TM mode light as a function of incident angle. This term is raised to the *2N* rather than *N* power as in Eq. [2] again because of the double pass nature of the fiber architecture. The relationships between the various angles and the integration angle are as follows:

$$\theta_i = \frac{\pi}{2} - \theta$$

$$\theta' = \sin^{-1}\left(\frac{n_2}{n_1}\sin\theta\right) \qquad [8]$$

$$\theta_t = \sin^{-1}\left(\frac{n_2}{n_{rr}}\cos\theta\right)$$

The reflectance function due to surface plasmon resonance (*r(θ)*) is given by the following:[7]

$$r(\theta) = \left|\frac{r_{21} + r_{130}e^{2ik_1d_1}}{1 + r_{21}r_{130}e^{2ik_1d_1}}\right|^2 \qquad [9]$$

where:

$$r_{130} = \frac{z_{10} - iz_{43}\tan(k_3d_3)}{n_{10} - in_{43}\tan(k_3d_3)}$$

$$r_{12} = \frac{z_{21}}{n_{21}}$$

$$z_{l,m} = k_l\varepsilon_m - k_m\varepsilon_l$$

$$n_{l,m} = k_l\varepsilon_m + k_m\varepsilon_l \qquad [10]$$

$$k_l = \left[\varepsilon_l\left(\frac{2\pi}{\lambda}\right)^2 - \left(\frac{2\pi}{\lambda}n_2\sin\theta\right)^2\right]^{1/2}, l = 1, 2, 3$$

$$\varepsilon_4 = \frac{\varepsilon_0\varepsilon_1}{\varepsilon_3}, \quad k_4 = \frac{k_0k_1}{k_3}$$

and the subscripts represent the layers as defined in Figure 2.

3. MODELING RESULTS:

A Mathcad[1] program was constructed to solve for the transmission through the optical system and vary the thickness parameters of the fibers based on the formalism above. Results were applied to choosing various thicknesses of metal films in order to locate the SPR minimum and estimate the response to various exposures. The results from the models in general do not exactly describe the measured behavior of the films tested; however, the general trends are described and employed to direct the sensor design.

Figure 3 is a plot of the calculated response of Pd to exposure to H_2 as given by the model and literature values of refractive index.[17,18] These simulations indicated that significant variations between pure Pd and PdH_x should be expected in the 200-400 nm range, which enables the detection of H_2. Calculations were done with 600 μm fiber with a numerical aperture of NA=0.22 and various thicknesses of PdH_x. These types of calculations were employed to direct the choice of metal thicknesses for the experimental studies but do not exactly model the position

[1] PTC, 140 Kendrick St., Needham, MA 02494 USA.

of the minimum response. In the example of Figure 3, various thicknesses of films were simulated in order to locate thicknesses that had substantial resonance peaks in the visible spectrum and could be easily fabricated. Similar studies were performed on Au/SiO_2 and Ag films.

4. EXPERIMENTAL

Preparation of the Fiber

Following the ray optics model described by Xu *et al*[7] the metal thickness was calculated for monitoring of H_2 using deposited Pd films, H_2S using Ag films, and moisture using a coverlayer of SiO_2 on an Au film. In addition, the core diameter of the optical fiber was chosen using this theoretical model. Figure 4 is a simulation for an Au film on a fiber of various core diameters from 100 μm to 1000 μm with the real and complex index of refraction components of Au plotted as a function of wavelength in the inset. The trend is for higher throughput and deeper SPR resonance minima as the core diameter becomes larger. However, in practice, 600 μm couplers are the largest conveniently available and therefore, fused quartz fiber of this diameter was chosen (Ocean Optics Fiber-600-UV[2]) for the experiment.

Sensing is accomplished by first etching off the cladding material and then coating a cylindrical section of the fiber with an SPR supporting metal film as illustrated in Figure 1. This geometry has the distinct advantage of doubling the sensitivity per unit length of the SPR film since the light travels through the sensitive section twice. In principal, multiple regions could be etched to the core and coated with different metals to vary the location of the SPR peak and allow sensing of several compounds using the same probe fiber.

Based on the results from the numerical simulations, a series of 600 μm core fibers were fabricated and coated with SPR supporting metals. The general process was to first cleave sections of optical fiber approximately 20 cm in length and then pyrolyze the last ~3 cm of the polyimide coating to allow the etching chemical access to the fused silica. The pyrolosis was accomplished by inserting the optical fiber in an alumina cylinder with a coil of nichrome wire wrapped around the cylinder and then using a power supply to heat the nichrome to incandescence. The fiber was then cleaned and etched by dipping the last 1.25 cm into a solution of 5 gm NH_4HF_2 dissolved in 50 ml deionized H_2O. The initial outside diameter of the fiber is 660 μm and the nominal core diameter is 600 μm; thus, the fibers were etched until they measured an outside diameter on the order of 590 nm to guarantee that the cladding had been completely removed and the core material alone was exposed. The measurement was accomplished using a digital micrometer.

Next, the fibers were rinsed in de-ionized water and then placed in a vacuum compatible rotating fixture. The fibers were then placed in an electron beam deposition system and pumped down to a base pressure of below $8x10^{-7}$ Torr. Next, they were coated with the respective SPR metal at rates of approximately 1 Å/sec for Pd, and Ag and a rate of 4 Å/sec for Au. The fibers were rotated at 3 RPM with a substrate temperature of ~24ºC until the quartz crystal thickness monitor indicated that the desired thickness was achieved. Finally, the fibers were then masked from the source except for the cleaved fiber end and the retro-reflecting coating was applied. In all cases, the retro-reflecting coating is a 100 nm Au film deposited using the same parameters as the SPR Au films. The thicknesses were verified using a stylus profilometer and found to be within ±20% of the nominal values.

[2] Ocean Optics, 830 Douglas Ave. Dunedin, FL 34698, USA

The responses of the fibers were then measured using the system depicted in Figure 1 and the data were analyzed. The system of Figure 1 consists of a tungsten-halogen light source (Ocean Optics LS-1) connected to a three port optical coupler (Ocean Optics 600 μm bifurcated fiber assembly). The spectrometer is an Ocean Optics USB-2000 system interfaced to a PC for data collection. An example of the raw data is shown in Figure 5 which illustrates the change in the spectral response as a function of exposure. The film in Figure 5 is a 30 nm Pd film deposited on ~1.25 cm of exposed fiber core. The dashed line spectrum is un-exposed film and the solid is the film hydrated in a partial pressure of ~0.2 Torr of H_2 in N_2. Since this is a large concentration, the effect is visible in the raw spectral data. However, in most cases the effect is small and must be extracted using numerical methods written in MATLAB.[3]

5. MATLAB ALGORITHMS

The MATLAB algorithm employed takes the spectrum from the unexposed fiber and averages several scans. This becomes the reference or background spectrum. All the scans are then normalized such that the maximum value is fixed at a value of unity. By doing this, effects such as light source aging, connector loss, and other drift mechanisms in the optical system are eliminated. This is key to application of this technique for long-term un-powered applications where it is neither practical nor desirable to continuously measure the spectrum. The rest of the data is then normalized to the beginning value and plotted as a function of time to look for trends in the spectral response of the fiber.

6. RESULTS

Pd/H2

Typical data for the Pd fiber is plotted in Figure 6 which illustrates the response of a 40 nm Pd film with a 100 nm Au retro-reflecting film exposed to various partial pressures of H_2 in N_2. The data at each wavelength has been normalized and then compared to its initial value. The data illustrate that at partial pressures below 200 mTorr, the response of the sensor is linear and the sign of the response is wavelength dependent. A linear response to H_2 at low concentrations has been reported previously for an SPR experiment in a Kirschmann configuration with a 633 nm light source.[19] It has been demonstrated that the linear trend continues over a sampling of wavelengths, but the absolute magnitude changes as a function of wavelength as well as the sign of the response. As illustrated in the graph, the response ceases to change as a function of concentration below about 70 mTorr corresponding to a signal-to-noise ratio of unity in the system. The predominant noise sources in the system are from the spectrometer. The spectrometer was set to average 20 scans with an integration interval of 100 msec.

Palladium hydride (PdH_x) forms for low partial pressures of H_2 in the α-phase. Transformation from the α-phase to the of β-phase of PdH_x occurs on exposure to higher concentrations of H_2 (15 to 20 Torr) where x~0.03 and is undesirable since it causes a 3.5% increase in the lattice spacing and will result in a mechanical failure of the Pd film on the fiber.[20] Our application is concerned with trace concentration of H_2 well below the β-phase, hence concentrations below 200 mTorr of H_2 partial pressure were tested.

Figure 7 is a plot of the measured response of a 40 nm Pd film exposed to H_2 plotted as a function of wavelength and as a function of scan number. Results demonstrate that the

[3] The MathWorks, Inc. 3 Apple Hill Drive, Natick, MA 01760-2098

measurement is strongly a function of wavelength with the maximum response wavelength in the same general wavelength region as was calculated using the model of Figure 3. In addition, the response is reversible and indicates the feasibility of using this technique for measurement of H_2 in a sealed environment.

Ag/H2S

Similar measurements have been conducted using Ag films exposed to 280 μTorr H_2S in N_2 for extended intervals of 7 days that demonstrate a non-reversible SPR response at wavelengths around 450 nm as compared to the maximum measured SPR response of Pd around 550 nm. These experiments were performed on the same 600 μm fiber coated with similar thicknesses of Ag. The shape of the spectrum is very similar to the data of Figure 7, with the SPR minimum translated approximately 100 nm shorter in wavelength.

SiO2/H2O

An additional system consisting of 20 nm of Au deposited on the fiber with a 20 nm cover layer of SiO_2 was used to monitor moisture changes in atmospheres with dew/frost points of 10˚C to -70˚C in N_2. The experimental results at around 550 nm to 600 nm show the most dramatic change in this moisture range and indicate that good discrimination between the spectra at -70˚C and -10˚C allows SPR measurements of moisture ingress in sealed systems using this SPR geometry.

The ability to measure several contaminants of interest and to discriminate between them by monitoring a series of key wavelengths implies that a single fiber with multiple regions etched and coated with different metals could be used to produce a multi-component sensor (Figure 8).

7. MULTI COATING SPR FIBER

Such a sensor has been demonstrated that was coated with 12.5 mm long 20 nm Pd film followed by a 12.5 mm length 20 nm Ag film followed by a 12.5 mm length 20 nm Au/20 nm SiO_2 film stack for detection of H_2, sulfur compounds, and moisture respectively (Figure 8). Data from these tests were first acquired using the unexposed fiber to detect 0.2 Torr H_2 (Figure 9 (a)) and then exposed to 300 μTorr of H_2S (Figure 9 (b)). The Ag section of the fiber was then monitored until the non-reversible reaction was complete. The fiber was then re-exposed to 0.2 Torr H_2 with the permanent H_2S/Ag response normalized into the data to determine if the sulfur atmosphere poisoned the Pd film (Figure 9 (c)). The data indicate that the resonance peak that appears on exposure to H_2 is essentially unchanged compared to Figure 9 (a) in shape and magnitude after the exposure of the Ag film to H_2S. It should be noted that Figure 9 (a) and (b) are normalized to the unexposed spectrum. Figure 9 (c) is re-normalized after the H_2S exposure and thus, includes the spectral features introduced on the exposure of the Ag film to H_2S. Since the two metals have non-overlapping surface plasmon resonances, the responses to the two analytes can be separately resolved. The resulting response indicated that low background levels of sulfur exposure for several days do not appreciably degrade the response of the Pd section to H_2. In all cases, a horizontal line at 1 would represent the reflectivity of the unexposed, normalized optical spectrum.

Figure 9 (d) is a plot of the response of the SiO_2/Au section of the fiber to drying from a frost point of 0˚C to -70˚C. This data illustrates that the moisture sensing section of the fiber is not poisoned by the H_2S and that monitoring of multiple components in the system is feasible by judicious choice of wavelengths in the SPR spectrum. The wavelength of maximum SPR response is similar in both the Pd and SiO_2/Au cases indicating that multiple wavelengths would

need to be monitored simultaneously to separate H_2O and H_2. Binary or ternary mixtures have not yet been tested using this approach.

8. CONCLUSIONS

Mathematical models to simulate the response of a fiberoptic-based surface plasmon resonance (SPR) sensor using a single fiber with a retro-reflective coating have been demonstrated. Several SPR supporting metals were then modeled and used to design sensors for testing including H_2 sensing using Pd films, H_2S sensing using Ag films, and H_2O sensing using SiO_2 films on an Au film. Data illustrate that different metals allow variation in the spectral response to various analyties allowing the manufacture of a three region SPR sensor that is sensitive to all three analytes using the single fiber and experimental system. It has been demonstrated that the H_2 response is unchanged after an extended interval of exposure to H_2S and that moisture can be detected at low frost points (-70 C) after repeated exposure to H_2 and prolonged exposure to H_2S. Thus, simplified fiber optic SPR geometry using a single-ended fiber has been demonstrated and shown to have multiple responses to several chemical vapors that can be present due to aging effects in sealed systems.

9. REFERENCES

1. S. Ekgasit, C. Thammacharoen, F. Yu, and W. Knoll, Appl. Spectrosc. **59**, 5, (2005).
2. I. Stemmler, A. Brecht, and G. Gauglitz, Sensors and Actuators: B, **54**, (1999).
3. P. T. Leung, D. Pollard-Knight, G. P. Malan, and M. F. Finlan, Sensors and Actuators: B,**22**, (1994).
4. C. M. Pettit and D. Roy, Analyst, **132**, (2007).
5. A. Ikehata, K. Ohara, and Y. Ozaki, Appl. Spectrosc. **62**, 5 (2008).
6. S. A. Love, B. J. Marquis, and C. L. Haynes, Appl. Spectrosc. **62**, 12, (2008).
7. Y. Xu, N. B. Jones, J. C. Fothergill, and C. D. Hanning, J. of Modern Optics, **47**, 6, (2000).
8. A. K. Sharma and B. D. Gupta, Sensors and Actuators: B, **100**, (2004).
9. M. Mitsushio, K. Miyashita, and M. Higo, Sensors and Actuators: B, **125**, (2006).
10. M. A. Butler and A. J. Ricco; Sensors and Actuators, **19** (1989.
11. M. A. Butler and A. J. Ricco; Appl. Phys. Lett. **53,** 16, (1988).
12. M. A. Butler, A. J. Ricco, and R. J. Baughman; J. Appl. Phys. **67,** 9, (1990).
13. K. B. Pfeifer, R. L. Jarecki, and T. J. Dalton; SPIE, **3539**, (1998).
14. B. E. A. Saleh and M. C. Teich, *Fundamentals of Photonics*, (John Wiles &Sons, Inc. New York, 1991), p.18.
15. W. L. Wolfe, *Introduction to Radiometry*, (SPIE Optical Engineering Press, Bellingham, WA 1998), p. 17.
16. E. Hecht and A. Zajac, *Optics*, (Addison Wesley, Reading MA, 1979), p. 74.
17. M. A. Ordal, L. L. Long, R. J. Bell, S. E. Bell, R. R. Bell, R. W. Alexander, and C. A Ward, Appl. Optics, **22**, 7, (1983).
18. K. V. Rottkay, M. Rubin, and P. A. Duine, J. Appl. Phys. **85**, 1, (1999).
19. B. Chadwick, J. Tann, M. Brungs, and M. Gal, Sensors and Actuators: B, **17**, (1994).
20. M. A. Butler, Appl. Phys. Lett., **45**, 10, (1984).

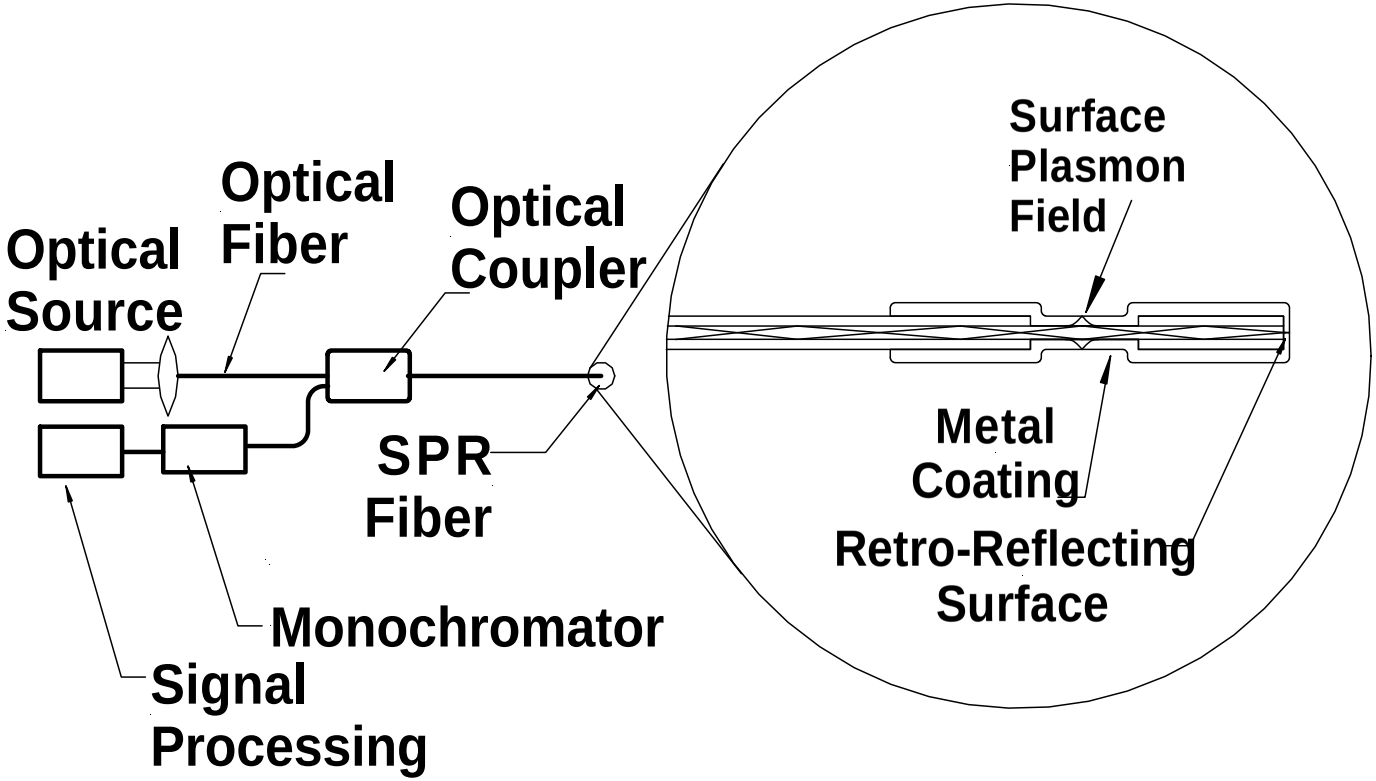

Figure **1.** Schematic diagram of the SPR sensor showing the optical system. Broad band light is injected into the fiber which then is sent to the SPR end via a three-port coupler. The light is passed through the SPR section of the fiber and reflected back by a retro-reflecting end back through the coupler and is detected by the monochromator.

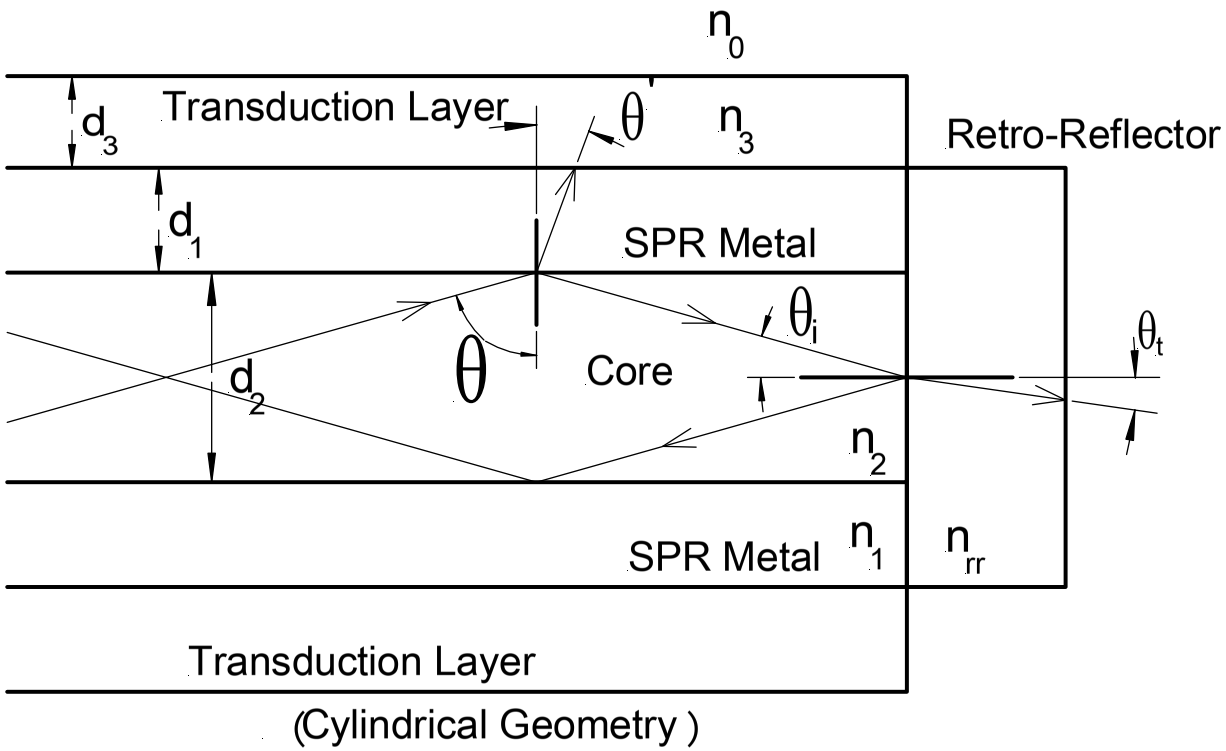

Figure 2. Diagram of geometry used to derive equations where the subscript 0 represents the outside atmosphere, 1 is the SPR supporting metal layer, 2 is the core, and 3 is an optional second transduction layer.

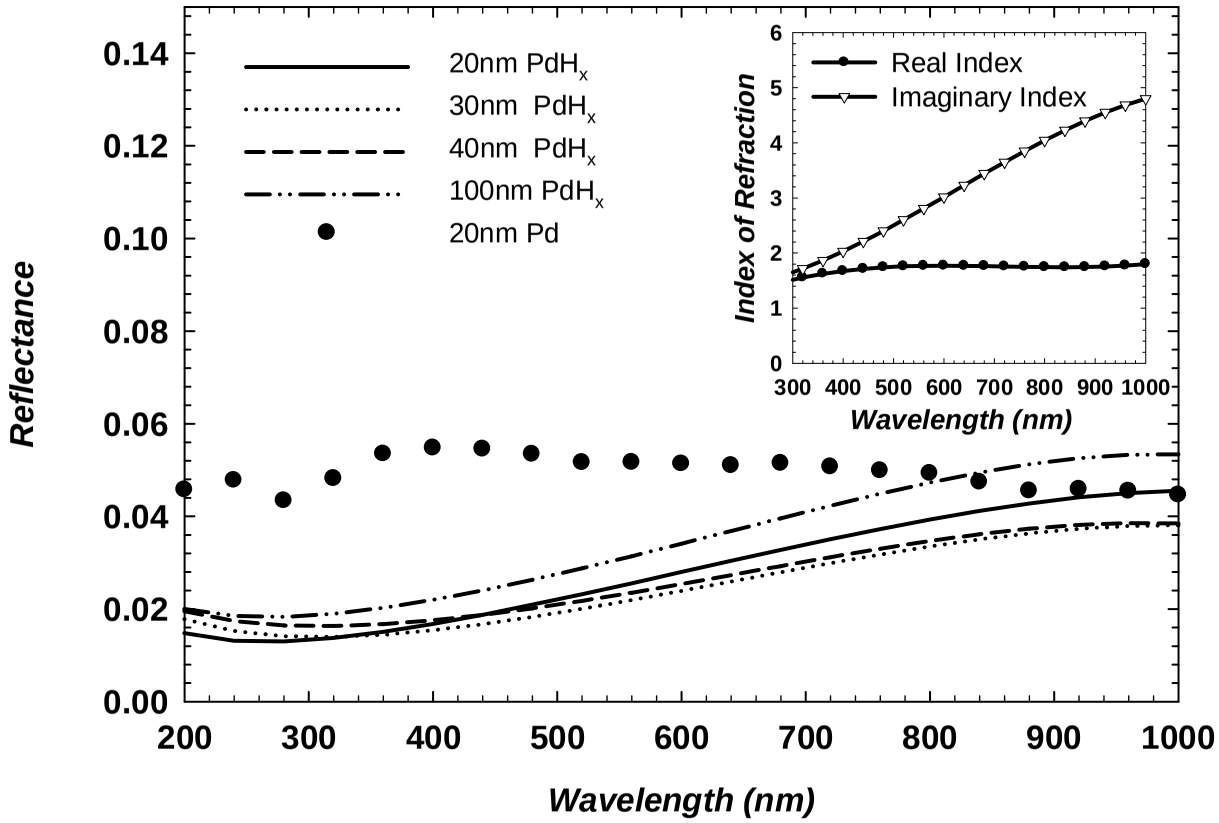

Figure 3. Plot of calculated reflectance for several thicknesses of Pd film exposed to H_2 to form PdH_x as calculated and compared to an unexposed 12.5 mm length, 20 nm thick Pd film in the SPR geometry. Data indicate that good candidates for fabrication and testing due to their broad absorption resonance being predicted in the 250-400 nm range are films with thicknesses of 20-40 nm . The real and imaginary parts of the index of refraction were obtained from the literature for PdH_x and are plotted in the inset graph.[17,18]

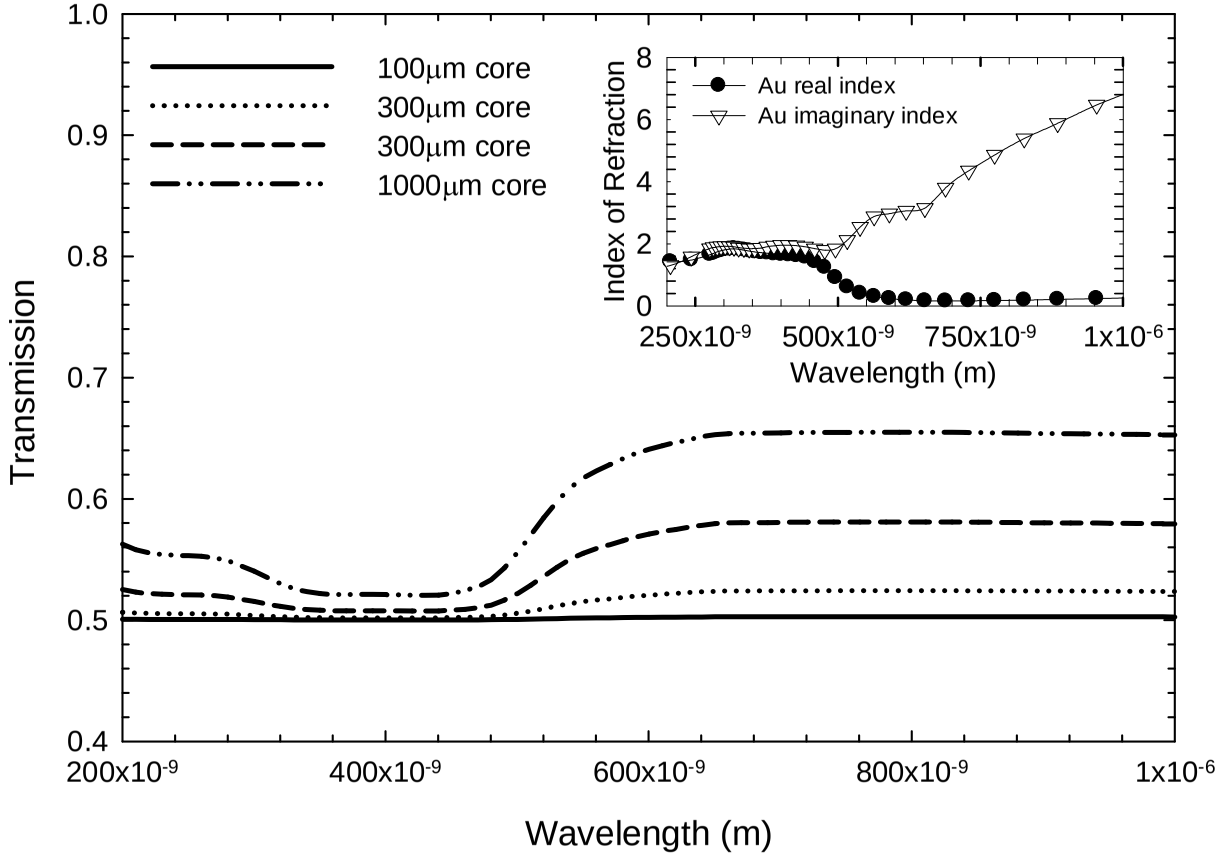

Figure 4. Plot of optical transmission for a 20 nm Au coated fiber as a function of wavelength for several different core diameters using the theory of Xu *et al.*[7] Plot illustrates that for SPR, the larger diameter gives a narrower SPR peak allowing more wavelength discrimination.

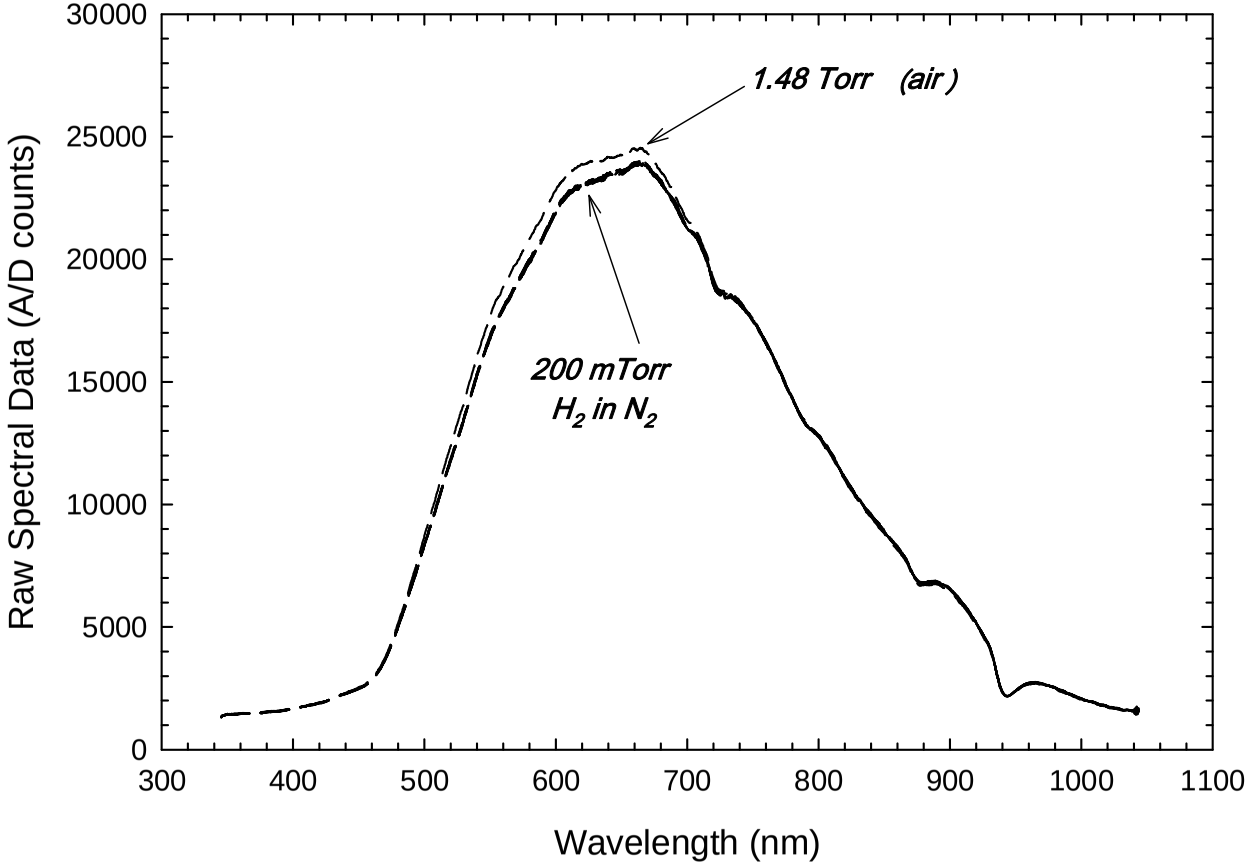

Figure 5. Plot of the raw spectral response from a 30 nm Pd coated fiber under conditions of near vacuum pumped from an air background and exposed to ~0.2 Torr of H_2.

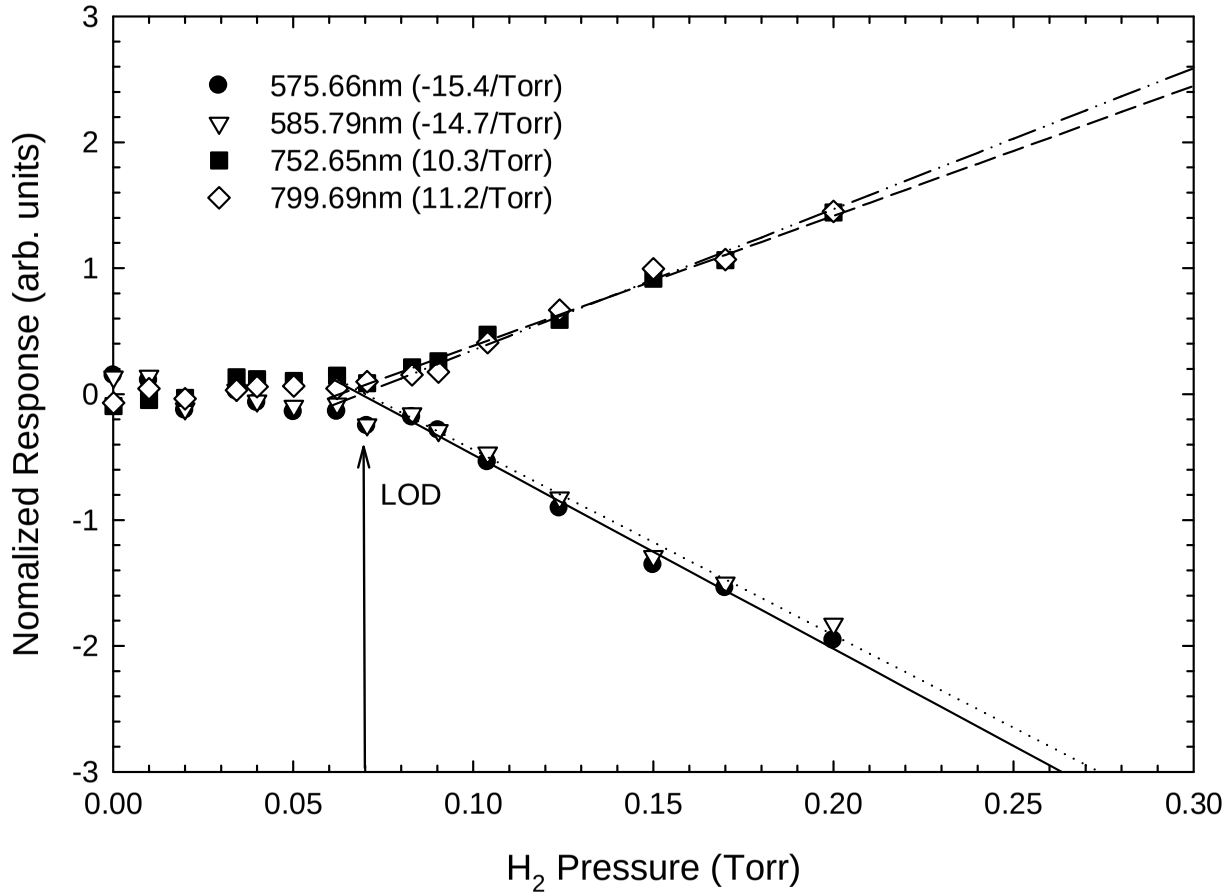

Figure 6. Plot of the normalized response of a 40 nm Pd film with a 100 nm Au retroreflector as a function of H_2 partial pressure at several wavelengths indicating that the sign of the response is wavelength dependent. Limit of detection on the order of 70 mTorr of H_2..

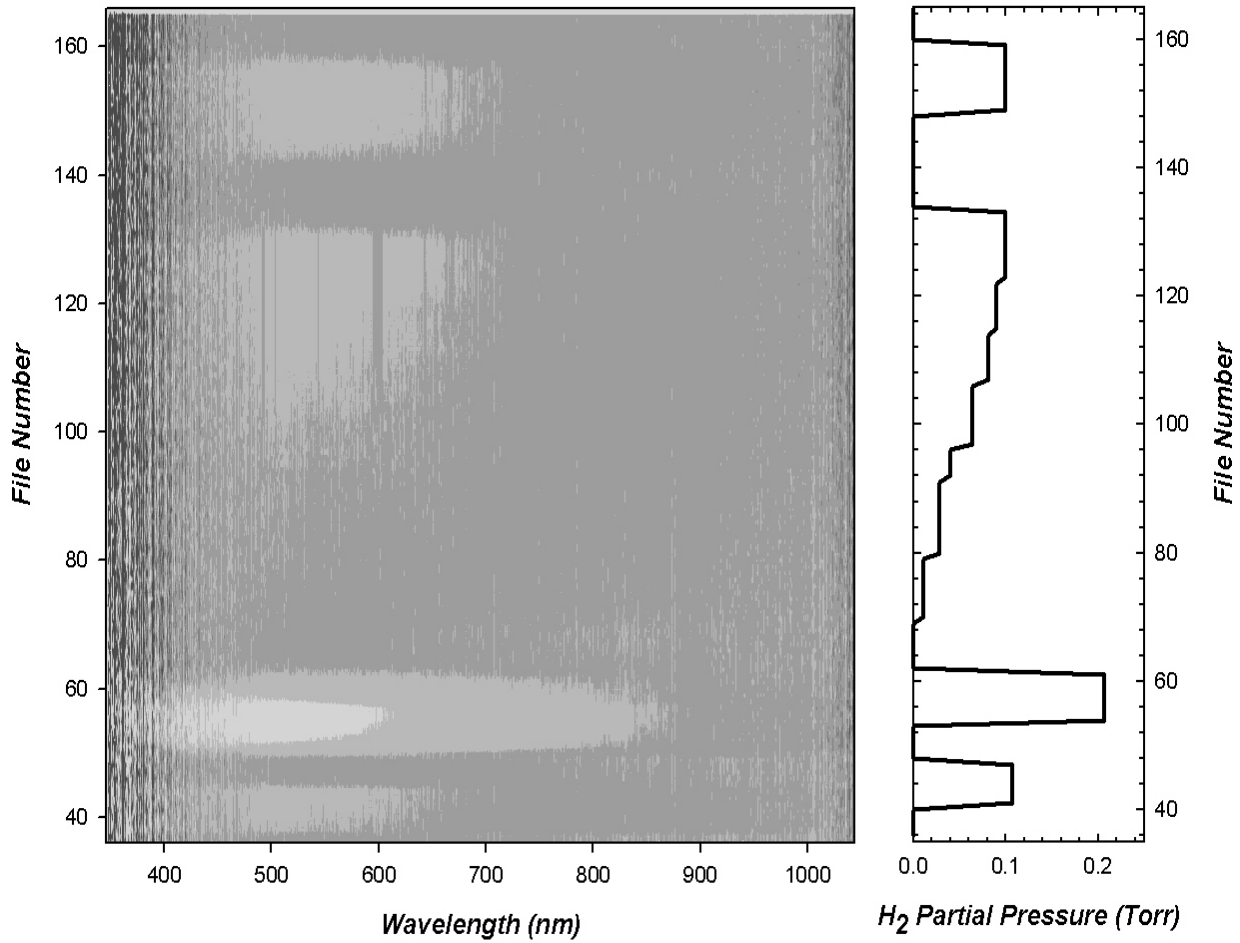

Figure 7. Plot of sensor response as a function of wavelength and scan time plotted along with the H2 partial pressure. Data illustrate that the sensor is reversible and has a strong dependence on wavelength as expected.

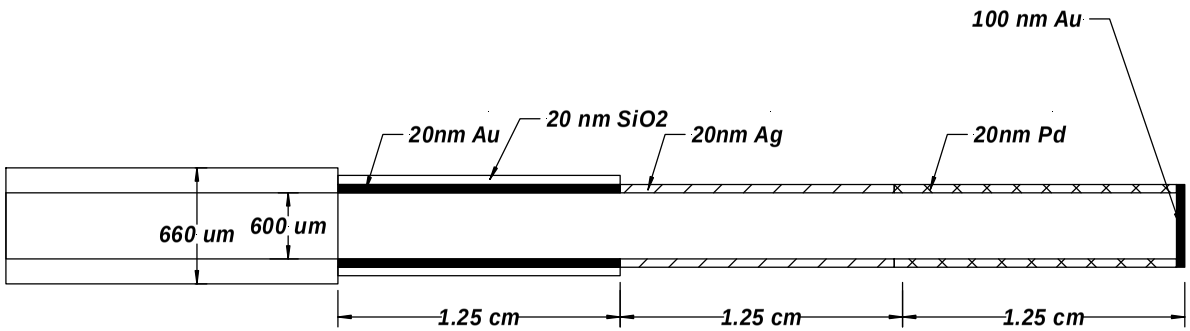

Figure 8. Diagram of three section SPR sensor showing Au, Ag, and Pd regions on a 600 µm optical fiber core.

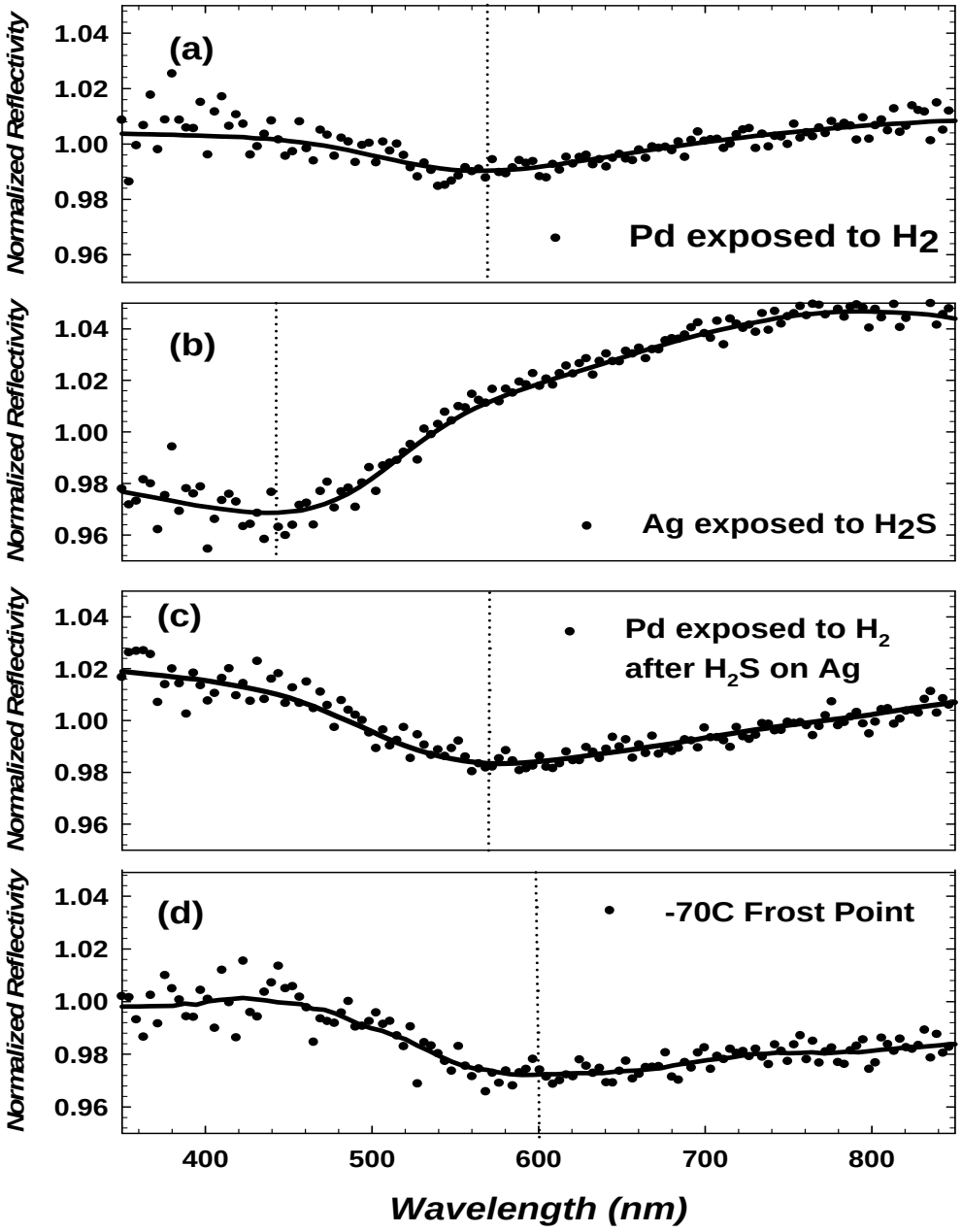

Figure 9. Plot showing the response to 200 mTorr H_2 in Pd (a), 280 μTorr H_2S on Ag (b), 200 mTorr H_2 in Pd (c), and drying the fiber from 0˚C frost point to -70˚C frost point (d) on a single SPR fiber. The time progression is from top to bottom and the data is re-normalized after the H_2S on Ag exposure since that change is not reversible. Thus, (c) and (d) are normalized to (b). The SPR wavelengths are separated with the minimum for Ag at approximately 450 nm, the minimum for Pd at about 550 nm, and the minimum for Au at about 600 nm. The dotted lines locate the minimum of the smoothed data.

10. DISTRIBUTION

5	MS1405	Kent B. Pfeifer	1717
5	MS0889	Steven M. Thornberg	1825
2	MS0889	Michael I. White	1825
2	MS1405	Arthur N. Rumpf	1717
2	MS1082	W. Kent Schubert	1717
2	MS0889	S. Jill Glass	1825
1	MS0899	Technical Library (electronic copy)	9536
1	MS0123	D. Chavez, LDRD Office	1011